Original Article
Circulating microRNAs, miR-10b-5p, miR-328-3p, miR-100 and let-7, are associated with osteoblast differentiation in osteoporosis

Ruisong Chen[1,2,3], Xin Liao[2], Fengrong Chen[2], Bowen Wang[2], Jianming Huang[2], Guojian Jian[2], Zheyuan Huang[2], Ganghui Yin[1,3], Haoyuan Liu[2], Dadi Jin[1,3]

[1]Department of Orthopedics, Third Affiliated Hospital of Southern Medical University, Guangzhou, Guangdong, PR China; [2]Department of Orthopedics, Chenggong Hospital Affiliated to Xiamen University (Department of Orthopedics, 174 Hospital of PLA), Xiamen, Fujian, PR China; [3]Orthopaedic Research Institute, Southern Medical University, Guangzhou, Guangdong, PR China

Abstract: Osteoporosis has become a major disease that threatened post-menopausal women and elder people. Circulating micorRNAs (miRNA) could provide useful information for diagnosis and therapeutics. The study employed RT-real time PCR to detect the circulating miRNAs between osteoporotic patients and healthy controls. Human and mouse osteoblast cell lines were used to test the differential induction effects by miRNAs. Alkaline phosphatase activity and Alizarin red staining were examined after miRNA mimics stimulation. The authors found 14 of 150 tested miRNAs were significantly aberrant expressed between patients and healthy controls. Results showed miR-328-3p, let-7g-5p, miR-133b, miR-22-3p, miR-2861, miR-518 miR-100 were down-regulated osteoporotic patient, while miR-10b-5p, miR-21, miR-125b and miR-127 were up-regulated. MiR-10b-3p, miR-328-3p, miR-100 and let-7 showed tight association with Wnt pathway. MiR-10b-5p increased ALP activity and mineral deposition in human and mouse osteoblast cells, indicating miR-10b-3p promoted osteoblast cell differentiation. MiR-328-3p and let-7g-5p decreased ALP activity and suppressed mineral deposition in both cell lines. Conclusively, miR-10b-5p promoted osteoblast cells differentiation; miR-328-3p, miR-100 and let-7 inhibited osteoblast cells differentiation.

Keywords: Osteoporosis, circulating miRNAs, osteoblast, differentiation, cell lines

Introduction

Osteoporosis is characterized by systemic skeletal disorder associated with deterioration of bone mass and microarchitecture [1]. Osteoblasts and osteoclasts make dynamic equilibrium of bone homeostasis. Cytokines deficiency becomes a major risk factor in osteoporosis in postmenopausal women, causing diminished osteoblast differentiation and maturation. Additionally, other investigators reminded that aberrant microRNAs (miRNAs) signatures might not be specific to the pathophysiology in bone, and indicated that more work remains to be done until the robust diagnostic biomarkers were established [2]. Despite these promising primary data, many studies demonstrated that miRNAs participated in bone formation, indicating the therapeutic roles of miRNAs in bone related diseases [3].

MiRNAs are a class of endogenous approximately 22 nucleotides, single chain and noncoding RNAs. MiRNAs participate in bone homeostasis through regulation of specific gene expression, such as Runx2 [4], and FGF2 [5]. It was reported that Osterix and miRNAs are involved in bone formation and Osterix-controlled osteogenesis [6]. Circulating miRNAs are regarded as special transporting miRNAs, which might have its specific function to nearby or long distance target cells. It was reported that osteoclasts-derived exosomes contain miRNAs, which target and inhibit osteoblasts activity and maturation [7]. New discoveries insight into the circulating miRNAs indicated circulating miRNAs after recent osteoporotic fractures can influence osteogenic differentiation [8]. Data implied circulating miRNAs can be taken up by cells and thereby influence the recipient cell's behavior in the context of diverse

Table 1. Summary of patients and controls characteristics

	Osteoporotic	SD	Control	SD
Number of samples	9	-	9	-
Age (years)	69.2	±2.7	67.1	±2.6
BMI (kg/m^2)	31.3	±1.5	33.4	±1.9
Vitamin D (μg/L)	21.2	±5.3	14.8	±3.6
PTH (ng/L)	49.4	±4.1	45.2	±5.8

biological functions [9]. In the aspect of biomarkers using miRNAs, measurability, validation and utility are realized as the fundamental bases of valuated biomarker for diagnosis. Because of noninvasive and easy sampling, circulating miRNAs have great potential to serve as biomarkers for osteoporosis [10]. Many therapeutic trials on osteoporosis and other bone related diseases using miRNAs have started in animal, indicating the age of miRNA therapy [11].

Many studies demonstrate that miRNAs can promote osteoblasts differentiation and participate in the regulation of differentiation [12]. A miRNAs cluster miR-23a~27a~24-2 regulated osteoblast differentiation, and connecting Runx2 and SATB2 in osteogenic cells [13]. In addition, miRNA also affect BMMSCs [14] and MSCs [15] in bone mass and density, providing a new strategy and insight for the treatment of osteoporosis. We realized miRNAs signature might not only serve as biomarkers, but also great potential as therapeutics drugs targeting osteoporosis. In the present study, we hypothesized that osteoporotic-specific miRNAs might be presented in serum as circulating biomarkers. These miRNAs was regarded as potential diagnostic biomarkers, however, it might be also used as promising drug targets. According to the above idea, we quantified the levels of 150 circulating miRNAs in serum samples from osteoporotic patients, and age-matched health controls from the affiliated hospital. This study aims to find the early diagnosis marker for osteoporosis using circulating miRNAs, as well as to explore the miRNA drug for osteoporosis therapeutics.

Materials and methods

Osteoporotic patients and healthy donor

Recruited osteoporotic patients were diagnosed in the university affiliated hospital, and agreed to join the current study. Patients were diagnosed medicine doctor under osteoporosis diagnostic BMD, CT results and other serological results. Healthy donors are persons who had routine physical examine in the hospital, and age- and sex-matched with patients. Included controls were without any obvious diseases, such as cold, chronic disease etc. Serum samples (9 patients and 9 controls) were collected and stored at -20 degree. This study was approved by The Ethical Committee of Southern Medical University (China), Referenced No.201605339.

RNA isolation

RNAs were extracted from cells using Trizol (Life sciences)-chloroform extraction and isopropanol precipitation method. 1 ml serum was mixed with 4 ml Trizol reagent and carried out exaction procedures following the manufactory's instructions. For good quality and safety, glycogen as a carrier at 1 μg/μl was also used (Thermo Scientific). Incubate the mixture for 5 minutes at room temperature, and add 0.8 mL of chloroform and incubate for 3 minutes at room temperature. Centrifuge the sample at 12,000 × g for 15 minutes at 4°C. Collect the RNA phase by angling the tube at 45° and pipetting the solution out. After twice wash with 70% EtOH, RNA pellets were air dried and resuspended in 50 μL of enzyme-free water. RNA concentration was analyzed by NanoDrop 2000 at 260 nm (Thermo Fisher). The RNA quality and purity were determined by 260/230 nm and 260/280 nm respectively.

Circulating microRNAs qPCR

Real-time PCR (RT-qPCR) quantification of circulating microRNAs was performed followed previous reported experiment [16]. Briefly, serum total RNA from RNA extraction step was used as template. MiRNAs real-time PCR reactions were performed using 96-well plate (Thermo Scientific). Firstly, 1 μg of total RNA was reverse transcribed using 20 μl reactions system by commercial kit (Thermo Scientific). After reversed transcription reaction, 2 μl PCR product was added for subsequent miRNA quantification in 10 μl reaction buffer system (Applied Biosystem). The reverse transcript primers and the real time PCR primers of four miRNAs were listed in Supplementary Table 1. U6 RNA and its primers were used as control.
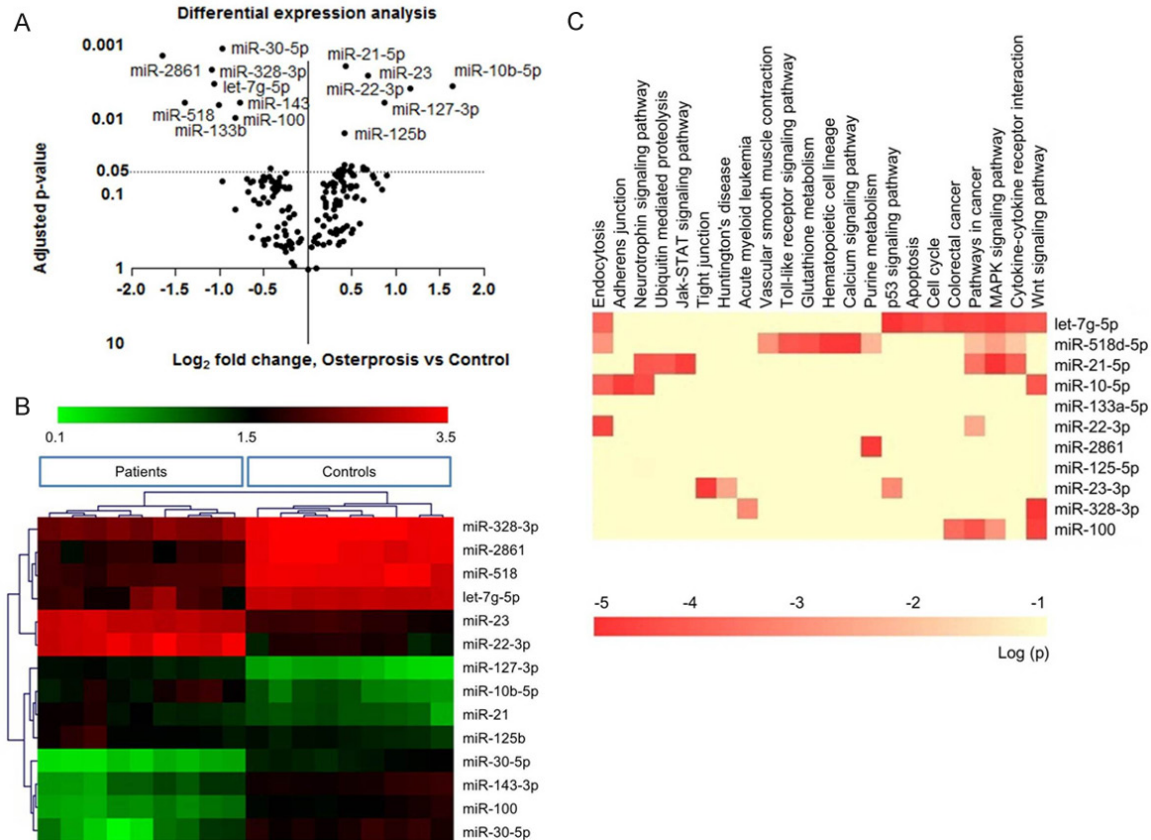
Figure 1. A: Volcanic chart showed aberrant expressed miRNAs among 150 tested circulating miRNAs. *P* value of paired t-test was used as y-axis, and Log2 (-2$^{\Delta ct}$) as x-axis. B: Real time PCR results showed down-regulated miRNAs in osteoporotic patient: let-7g-5p, miR-133b, miR-328-3p, miR-22-3p, miR-2861, miR518, and up-regulated miR-10b-5p, miR-21, miR-125b, miR-23 and miR-100. C: Clustering of these miRNAs correctly classify osteoporotic patients and healthy controls. Heatmap of KEGG pathways enriched from 14 miRNAs target genes was plotted. The 14 miRNAs were involved in multiple pathways, especially Wnt pathway, bone metabolic, cell growth and differentiation pathway.

MiRNA PCR was carried out at 94°C for 30 s, 55°C for 30 s and 72°C for 45 s for 30 cycles, using ABI prism 7700 sequence detector and software to analyze the data (Applied Biosystems, CA).

Cell culture

Human osteoblast cells hFOB1.19 (cat: CRL-11372™) and mouse osteoblast cells MC-3T3-E1 were purchased from American Type Culture Collection (ATCC). hFOB1.19 cells were cultured with complete growth medium, for quick growth setting the temperature at 33.5°C, for differentiation and maturation analysis setting the culture temperature at 39.5°C, with 5% CO$_2$ in humidity air incubator. The complete growth culture medium contains 10% fetal bovine serum (Gibco), 1 ng/ml recombi-

nant human basic fibroblast growth factor (human FGF, Peprotech) and 4 mM L-glutamine in HAM's F-12 medium (Gibco, Thermo). MC3T3-E1 was cultured with Alpha Minimum Essential Medium supplement with 2 mM L-glutamine and 1 mM sodium pyruvate, and 10% fetal bovine serum. Cell culture condition was 37°C, with 5% CO$_2$ in humidity air. Cells were passaged when the density was up to 85% at a split ratio of 1:3.

Alkaline phosphatase assay

In order to quantify the activity of alkaline phosphatase (ALP), culture medium was aspirated and cells were lysed in 100 µL ALP lysis buffer (0.25% v/v Triton X-100 in 0.5 M 2-amino-2-methyl-1-propanol, 2.0 mM magnesium chloride (Sigma-Aldrich). Seven days after treatment

Table 2. Detail KEGG pathway analysis of 4 miRNAs

| miRNA	Term	Count	p Value	Genes
mir-10b	hsa04310:Wnt signaling pathway	3	0.0018	CTNNBIP1, MAP3K7, CAMK2B
	hsa04520:Adherens junction	3	0.0058	MAP3K7, ACTG1, SSX2IP
	hsa04722:Neurotrophin signaling pathway	3	0.0131	BDNF, PIK3CA, CAMK2B
	hsa04144:Endocytosis	3	0.0242	SMAP1, TFRC, NEDD4
let-7	hsa04115:p53 signaling pathway	4	0.0053	CCND2, TP53, FAS, MDM4
	hsa04010:MAPK signaling pathway	5	0.005	TGFBR1, DUSP16, TP53, FAS, NGF
	hsa04310:Wnt signaling pathway	3	0.0191	CCND2, TP53, FZD3
	hsa05210:Colorectal cancer	3	0.0073	TGFBR1, TP53, FZD3
	hsa04210:Apoptosis	3	0.0077	TP53, FAS, NGF
	hsa05200:Pathways in cancer	5	0.0092	TGFBR1, TP53, FZD3, ZBTB16, FAS
	hsa04110:Cell cycle	3	0.0141	CCND2, TP53, CDC25A
	hsa04060:Cytokine-cytokine receptor interaction	4	0.016	TGFBR1, FAS, TNFSF9, CCL7
	hsa04144:Endocytosis	3	0.0256	PARD6B, ADRB2, TGFBR1
miR-328	hsa04310:Wnt signaling pathway	3	0.0212	CTNNBIP1, CHP2, TCF7L2
	hsa05221:Acute myeloid leukemia	3	0.0043	EIF4EBP1, PIM1, TCF7L2
	hsa05412:Arrhythmogenic right ventricular cardiomyopathy (ARVC)	3	0.0069	ITGA9, ITGA5, TCF7L2
	hsa04810:Regulation of actin cytoskeleton	3	0.0349	ITGA9, ITGA5, WASF2
miR-100	hsa05200:Pathways in cancer	5	0.0017	IGF1R, FZD8, FGFR3, MTOR, FZD5
	hsa05210:Colorectal cancer	3	0.0028	IGF1R, FZD8, FZD5
	hsa04114:Oocyte meiosis	3	0.0046	IGF1R, PPP3CA, PPP1CB
	hsa04010:MAPK signaling pathway	4	0.0048	FGFR3, RASGRP3, TAOK1, PPP3CA
	hsa00534:Heparan sulfate biosynthesis	2	0.0079	HS3ST2, HS3ST3B1
	hsa04310:Wnt signaling	3	0.008	FZD8, PPP3CA, FZD5
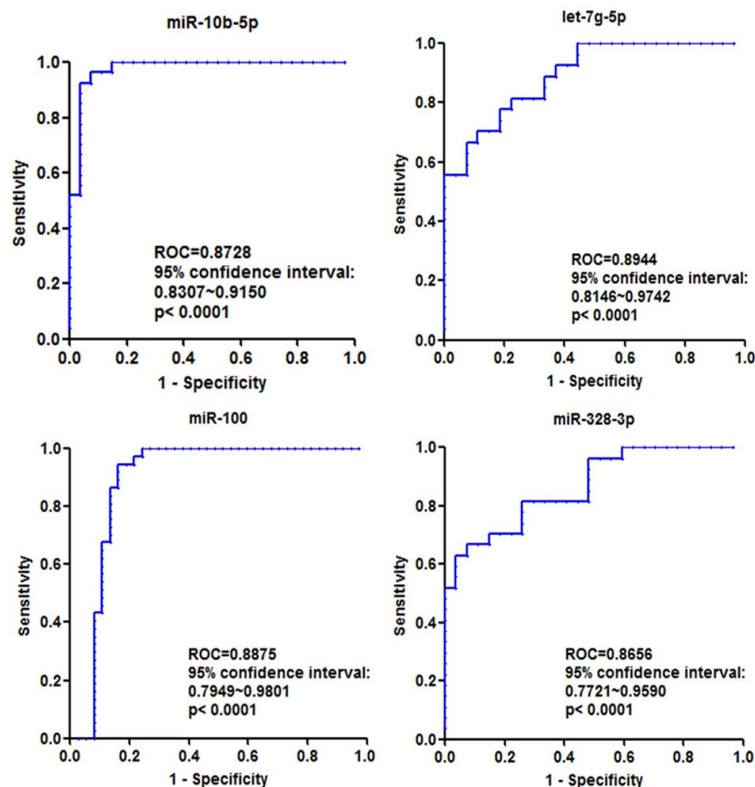
Figure 2. ROC curves analysis of each miRNAs to dichotomize healthy control and osteoporosis patient. The ROC area of patient related miRNAs are over 0.85, which are quite a sensitive and specific marker for osteoporosis diagnosis (all comparison are P<0.001).

of osteogenesis induction and miRNAs treatment. After centrifuge with 13,000 × g for 10 min, collect the supernatant, and add 50 µL ALP Buffer A, and incubate for 20 min at room temperature. Finally, stop reaction by 50 µL NaOH (0.2 M). The absorption at 405 nm was measured, setting reference absorbance at 620 nm [8]. Quantification of ALP activity was performed using human and mouse osteoblast cell lines and 4 independent replicate wells each.

Alizarin red staining

Alizarin red staining experiment was carried out to show the efficacy of calcium mineralization. MiRNA transfected cells were fixed in 70% ethanol for 1 h, followed by wash with PBS twice. Cells were stained with 50 mM Alizarin Red solution for 20 min (Sigma). Wash the cells until unbound dye was
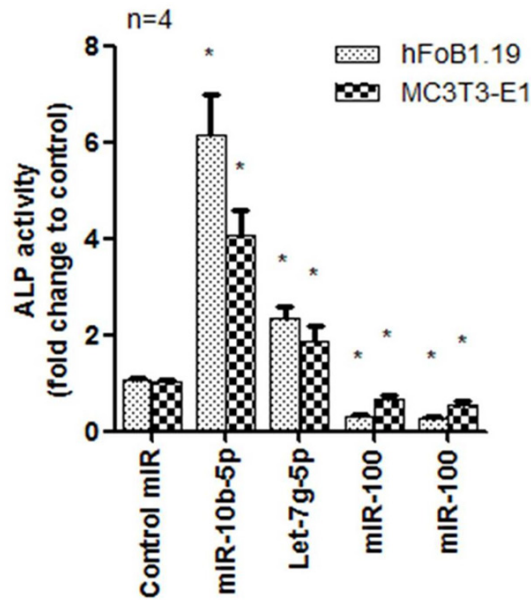
Figure 3. Detection of ALP activity in human and mouse osteoblast cells using miR-10b-3p, miR-328-3p and let-7g-5p. Data showed that miR-10b-3p promoted cell.

removed. Observe and count the positive nudes under microscopy.

Statistical analysis

MiRNA expression level comparison in paired patients and healthy controls was used U-test method. In ALP activity and alizarin red staining experiments, U-test method was applied. In four miRNAs ROC dichotomization, t-test was used as default method. Data are presented as mean ± standard derivation, unless stated otherwise. All the statistical comparisons were used SPSS 13.0 software. ROC curve analysis was performed by Prism 5.0 software, and its statistical analysis method. Statistical significance was achieved when the *p* value is <0.05.

Results

Biostatistical analysis identified 14 differentially expressed circulating miRNAs in osteoporotic patients with age-matched healthy controls

The study was approved by the Xiamen University Ethic Committee Conference. All patients and age-matched healthy controls agreed with study content and signed the agreement form. Detail information was listed in **Table 1**. We performed RT-real time PCR to detect the circulating miRNAs between osteoporotic patients and healthy controls, and clustered the differential miRNAs against patients and controls. *P* value of paired t-test was used as y-axis, and Log2 (-2$^{\Delta ct}$) as x-axis (**Figure 1A**). Among 150 tested miRNAs, 14 of them were significantly aberrant expressed. as showed in volcanic chart (**Figure 1B**). Results showed down-regulated miRNAs in osteoporotic patient: let-7g-5p, miR-133b, miR-328-3p, miR-22-3p, miR-2861, miR518, and up-regulated miR-10b-5p, miR-21, miR-125b, miR-23 and miR-100.

Identification of selected miRNAs in osteoblast differentiation

We predicted potential targets of each miRNA using online software (www.targetscan.org/vert_71/). Predicted targets were listed in Supplementary Table 2. We put the miRNA targets for KEGG pathway analysis one by one, for the purpose of miRNA involved signal pathway. Heatmap of KEGG pathways enriched from 14 miRNA target genes was plotted. The 14 miRNAs were involved in multiple pathways, especially Wnt pathway, bone metabolic, cell growth and differentiation pathway (**Figure 1C**). Additionally, miR-10b-3p, miR-328-3p, miR-100 and let-7 showed tight association with Wnt pathway (**Table 2**).

ROC curve analysis of four miRNAs in osteoporosis diagnosis

In order to explore the sensitivity and specificity of these four miRNAs in prediction of osteoporosis, we use ROC curve method to analyze the data using Prism software 5.0. Results showed that the sensitivity and specificity of miRNAs were quite high, specially, ROC area of let-7g-3p was up to 0.8944, with 95% confidence from 0.8146 to 0.9742 (**Figure 2**). Therefore, we could draw a conclusion that these four miRNAs are very potential for osteoporosis diagnosis, and further study is required to enlarge the sample size.

miRNA mimics increase ALP activity and Alizarin red staining

We found miR-10b-5p which was up-regulated in osteoporotic patients could increase ALP activity in human and mouse osteoblast cells, indicating miR-10b-3p promoted osteoblast
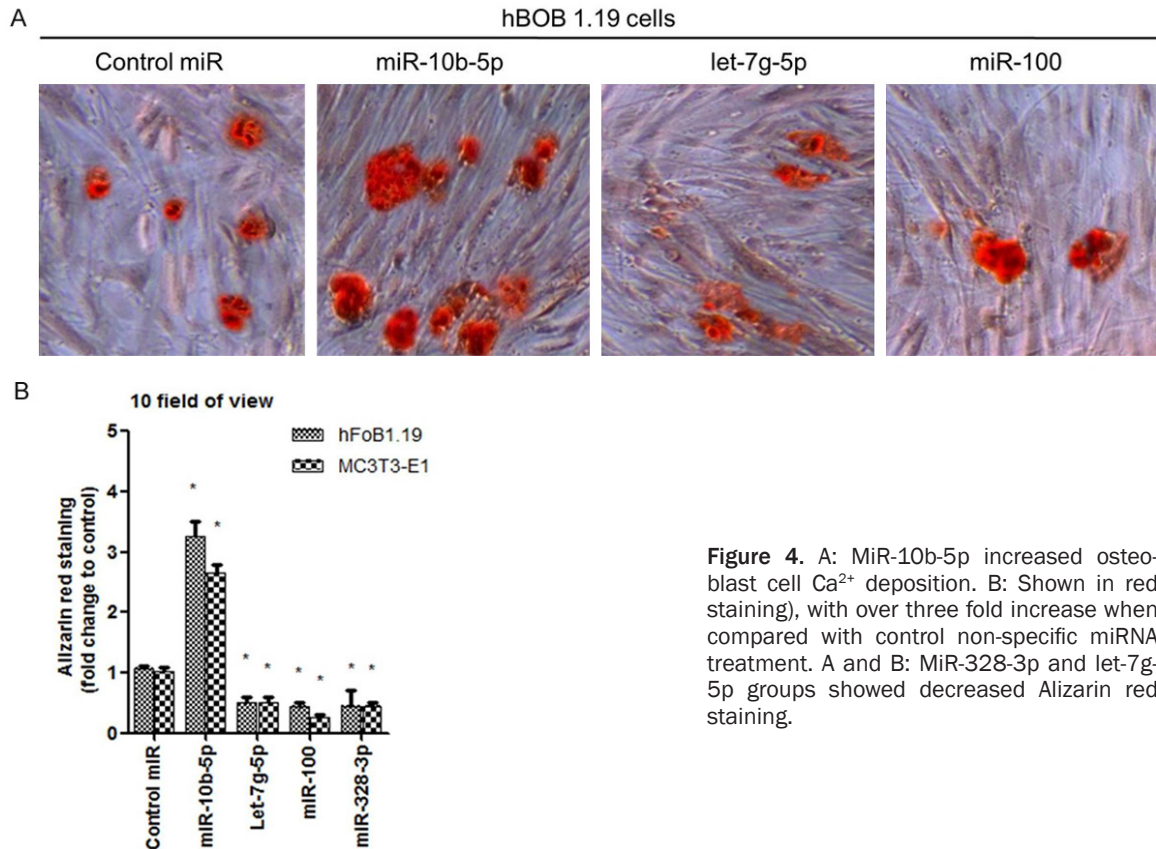
Figure 4. A: MiR-10b-5p increased osteoblast cell Ca^{2+} deposition. B: Shown in red staining), with over three fold increase when compared with control non-specific miRNA treatment. A and B: MiR-328-3p and let-7g-5p groups showed decreased Alizarin red staining.

cell differentiation (**Figure 3**). miR-328-3p and let-7g-5p decreased ALP activity in both cell lines. The above miRNAs are involved in Wnt pathway, but it seems that their functions in cell differentiation are different. In order to make clear the role of three miRNAs in osteoblast differentiation, we explore if they can increase Ca^{2+} deposition in osteoblast cell which is a maturation marker of osteoblast cell. We used Alizarin red to stain the positive cell. Results showed miR-10b-5p increased over three fold positive staining compared with control miRNA (**Figure 4A** and **4B**). miR-328-3p and let-7g-5p groups showed decreased Alizarin red staining (**Figure 4A** and **4B**).

Discussion

Many studies focused on circulating miRNAs in the aims of diagnostic biomarkers development [17, 18]. Our findings showed the unique circulating miRNAs based on peers' studies and further validated the function of interested miRNAs. In agreement with Weilner's study [8] of let-7g-5p, miR-328, miR-127 et al., they are differentially expressed as potential biomark-

ers, but we showed miR-10b-5p, miR-22, and miR-100 which are reversed expressed, meet with Trompeter's study [19], and Zeng's study [20]. In this aspect, we think osteoporotic patients need further detailed classification using statistic-based criteria. This study indicated the important role of aberrant miRNAs which could discriminate patients and healthy controls. The four miRNAs are associated with Wnt pathway which is vital in osteoblasts differentiation and maturation, especially bone homeostasis [21, 22].

The newest study revealed that secreted miR-214 inhibited osteoblast activity [7], and showed that circulating miRNAs were capsulated in exosomes, which were a double layer lipid membrane particles. The study implies that miRNAs act as a message to deliver inhibitory signal form osteoclasts to osteoblasts, and such miRNAs was also a promising therapeutic target for osteoporosis [23]. Similarly, another study found mouse MC3T3-E1 cells secreted exosomes promoted bone marrow stromal cell (ST2) to differentiate to osteoblast [24]. Study showed that 1,25 D effect on human HOB cells

was not restricted to classical VDR-mediated transcriptional responses but also involved in miRNA-directed posttranscriptional mechanisms [25]. But the study has not revealed if the osteoblast-secreted exosomes contained miRNAs. Study revealed a new cell-cell communication form using exosome materials. The secreted exosomes might benefit or damage bone mass based on the current point of view. Only have we made clear what was contained in the exosomes and the specific targets, the diagnostic and therapeutic miRNAs might come real. We found the diagnostic role of circulating miRNA, miR-10b-5p, miR-328, miR-100 and let-7 in osteoporotic patients, and characterized their function in osteoblast cell maturation. Increased miR-10b-5p stimulated human and mouse pre-osteoblast cells' maturation. Therefore, we hypothesize that these circulating miRNAs might be also capsuled in exosomes secreted by osteoblast or osteoclasts. The idea needs further exploration and validation. Limited by the current findings, we did not have direct evidences to validate this idea. In future study, electron microscopy should be employed to visualize these miRNA-containing exosomes in serum, and to identify the specific exosomes secreted by osteoblasts or osteoclast.

Kyoto Encyclopedia of Genes and Genomes (KEGG, http://www.genome.jp/kegg/) analysis automatically showed the related pathway of input genes. In this study, KEGG pathway was performed after potential regulated genes of miRNAs were predicted. Although the results from KEGG analysis were just possible data, it was meaningful and indicative for the subsequent study. Four miRNAs, miR-10b-5p, miR-328, miR-100 and let-7, showed significant association with Wnt pathway (P<0.001), which was regarded playing vital role in osteoblast maturation and bone mass formation [26]. The results remind us that circulating miRNAs have their specific function and targets. Therefore, we carried out the ALP activity assay and Ca^{2+} mineralization experiments in study, because these experiments indicate osteoblast maturation and bone mass formation. In peers' studies, Thorfve and colleagues used KEGG analysis to identify Wnt pathway markers in Osteoarthritic Cartilage [27]; Wei et al. reported that they identified 33 risk pathways and enriched GWAS variants using KEGG analysis

[28]; Gong et al. revealed Satb2-induced osteogenic differentiation finally, based on differentially regulated miRNAs using KEGG analysis [29]. KEGG pathway analysis, specially, for miRNAs potential targets, helps to achieve maximum results with little effort in the study.

Disclosure of conflict of interest

None.

Address correspondence to: Dr. Haoyuan Liu, Department of Orthopedics, Chenggong Hospital Affiliated to Xiamen University, Xiamen 361003, Fujian, PR China. Tel: +86 592 6335707; Fax: +86 592 6335707; E-mail: haoyuan.liu.xu@foxmail.com; Dr. Dadi Jin, Department of Orthopedics, Third Affiliated Hospital of Southern Medical University, 183 West Zhongshan Road, Guangzhou 510665, Guangdong, PR China. Tel: +86 20 38252295; Fax: +86 20 38252295; E-mail: jinda_di@yahoo.com

References

[1] Kanis JA, McCloskey EV, Johansson H, Cooper C, Rizzoli R, Reginster JY; Scientific Advisory Board of the European Society for C, Economic Aspects of O, Osteoarthritis and the Committee of Scientific Advisors of the International Osteoporosis F. European guidance for the diagnosis and management of osteoporosis in postmenopausal women. Osteoporos Int 2013; 24: 23-57.

[2] Hackl M, Heilmeier U, Weilner S and Grillari J. Circulating microRNAs as novel biomarkers for bone diseases-complex signatures for multifactorial diseases? Mol Cell Endocrinol 2016; 432: 83-95.

[3] Papaioannou G, Mirzamohammadi F and Kobayashi T. MicroRNAs involved in bone formation. Cell Mol Life Sci 2014; 71: 4747-4761.

[4] Zhang Y, Xie RL, Croce CM, Stein JL, Lian JB, van Wijnen AJ and Stein GS. A program of microRNAs controls osteogenic lineage progression by targeting transcription factor Runx2. Proc Natl Acad Sci U S A 2011; 108: 9863-9868.

[5] Lei SF, Papasian CJ and Deng HW. Polymorphisms in predicted miRNA binding sites and osteoporosis. J Bone Miner Res 2011; 26: 72-78.

[6] Chen Q, Liu W, Sinha KM, Yasuda H and de Crombrugghe B. Identification and characterization of microRNAs controlled by the osteoblast-specific transcription factor Osterix. PLoS One 2013; 8: e58104.

[7] Sun W, Zhao C, Li Y, Wang L, Nie G, Peng J, Wang A, Zhang P, Tian W, Li Q, Song J, Wang C, Xu X, Tian Y, Zhao D, Xu Z, Zhong G, Han B, Ling

S, Chang YZ and Li Y. Osteoclast-derived microRNA-containing exosomes selectively inhibit osteoblast activity. Cell Discov 2016; 2: 16015.

[8] Weilner S, Skalicky S, Salzer B, Keider V, Wagner M, Hildner F, Gabriel C, Dovjak P, Pietschmann P, Grillari-Voglauer R, Grillari J and Hackl M. Differentially circulating miRNAs after recent osteoporotic fractures can influence osteogenic differentiation. Bone 2015; 79: 43-51.

[9] Zhu H and Fan GC. Extracellular/circulating microRNAs and their potential role in cardiovascular disease. Am J Cardiovasc Dis 2011; 1: 138-149.

[10] Seeliger C, Karpinski K, Haug AT, Vester H, Schmitt A, Bauer JS and van Griensven M. Five freely circulating miRNAs and bone tissue miRNAs are associated with osteoporotic fractures. J Bone Miner Res 2014; 29: 1718-1728.

[11] Nakasa T, Yoshizuka M, Andry Usman M, Elbadry Mahmoud E and Ochi M. MicroRNAs and bone regeneration. Curr Genomics 2015; 16: 441-452.

[12] Wang H, Sun Z, Wang Y, Hu Z, Zhou H, Zhang L, Hong B, Zhang S and Cao X. miR-33-5p, a novel mechano-sensitive microRNA promotes osteoblast differentiation by targeting Hmga2. Sci Rep 2016; 6: 23170.

[13] Hassan MQ, Gordon JA, Beloti MM, Croce CM, van Wijnen AJ, Stein JL, Stein GS and Lian JB. A network connecting Runx2, SATB2, and the miR-23a~27a~24-2 cluster regulates the osteoblast differentiation program. Proc Natl Acad Sci U S A 2010; 107: 19879-19884.

[14] Wang C, Meng H, Wang X, Zhao C, Peng J and Wang Y. Differentiation of bone marrow mesenchymal stem cells in osteoblasts and adipocytes and its role in treatment of osteoporosis. Med Sci Monit 2016; 22: 226-233.

[15] Li C, Wei G, Gu Q, Wang Q, Tao S and Xu L. Proliferation and differentiation of rat osteoporosis mesenchymal stem cells (MSCs) after telomerase reverse transcriptase (TERT) transfection. Med Sci Monit 2015; 21: 845-854.

[16] Gimondi S, Dugo M, Vendramin A, Bermema A, Biancon G, Cavane A, Corradini P and Carniti C. Circulating miRNA panel for prediction of acute graft-versus-host disease in lymphoma patients undergoing matched unrelated hematopoietic stem cell transplantation. Exp Hematol 2016; 44: 624-634.e1.

[17] Garnero P. New developments in biological markers of bone metabolism in osteoporosis. Bone 2014; 66: 46-55.

[18] Zhang L, Xu Y, Jin X, Wang Z, Wu Y, Zhao D, Chen G, Li D, Wang X, Cao H, Xie Y and Liang Z. A circulating miRNA signature as a diagnostic biomarker for non-invasive early detection of breast cancer. Breast Cancer Res Treat 2015; 154: 423-434.

[19] Trompeter HI, Dreesen J, Hermann E, Iwaniuk KM, Hafner M, Renwick N, Tuschl T and Wernet P. MicroRNAs miR-26a, miR-26b, and miR-29b accelerate osteogenic differentiation of unrestricted somatic stem cells from human cord blood. BMC Genomics 2013; 14: 111.

[20] Zeng Y, Qu X, Li H, Huang S, Wang S, Xu Q, Lin R, Han Q, Li J and Zhao RC. MicroRNA-100 regulates osteogenic differentiation of human adipose-derived mesenchymal stem cells by targeting BMPR2. FEBS Lett 2012; 586: 2375-2381.

[21] Rauner M, Rachner TD and Hofbauer LC. Bone formation and the Wnt signaling pathway. N Engl J Med 2016; 375: 1902.

[22] Xie W, Ji L, Zhao T and Gao P. Identification of transcriptional factors and key genes in primary osteoporosis by DNA microarray. Med Sci Monit 2015; 21: 1333-1344.

[23] Liu X, Zhao J, Liu Q, Xiong X, Zhang Z, Jiao Y, Li X, Liu B, Li Y and Lu Y. MicroRNA-124 promotes hepatic triglyceride accumulation through targeting tribbles homolog 3. Sci Rep 2016; 6: 37170.

[24] Cui Y, Luan J, Li H, Zhou X and Han J. Exosomes derived from mineralizing osteoblasts promote ST2 cell osteogenic differentiation by alteration of microRNA expression. FEBS Lett 2016; 590: 185-192.

[25] Lisse TS, Chun RF, Rieger S, Adams JS and Hewison M. Vitamin D activation of functionally distinct regulatory miRNAs in primary human osteoblasts. J Bone Miner Res 2013; 28: 1478-1488.

[26] Karner CM and Long F. Wnt signaling and cellular metabolism in osteoblasts. Cell Mol Life Sci 2017; 74: 1649-1657.

[27] Thorfve A, Dehne T, Lindahl A, Brittberg M, Pruss A, Ringe J, Sittinger M and Karlsson C. Characteristic markers of the WNT signaling pathways are differentially expressed in osteoarthritic cartilage. Cartilage 2012; 3: 43-57.

[28] Wei J, Li M, Gao F, Zeng R, Liu G and Li K. Multiple analyses of large-scale genome-wide association study highlight new risk pathways in lumbar spine bone mineral density. Oncotarget 2016; 7: 31429-31439.

[29] Gong Y, Xu F, Zhang L, Qian Y, Chen J, Huang H and Yu Y. MicroRNA expression signature for Satb2-induced osteogenic differentiation in bone marrow stromal cells. Mol Cell Biochem 2014; 387: 227-239.

Supplementary Table 1. Primers for reverse transcription and real-time PCR of miRNA

miRNA	Reverse transcript PCR primer	Forward	Reverse
miR-10b-5p	GTCGTATCCAGTGCAGGGTCCGAGGTATTCGCACTGGATACGACCACAAA	TACCCTGTAGAACCGAATT	GTGCAGGGTCCGAGGT
miR-328-3p	GTCGTATCCAGTGCAGGGTCCGAGGTATTCGCACTGGATACGACACGGAA	CTGGCCCTCTCTGCCCTT	GTGCAGGGTCCGAGGT
miR-100	GTCGTATCCAGTGCAGGGTCCGAGGTATTCGCACTGGATACGACCACAAG	AACCCGTAGATCCGAACT	GTGCAGGGTCCGAGGT
let-7g-5p	GTCGTATCCAGTGCAGGGTCCGAGGTATTCGCACTGGATACGACAACTGT	TGAGGTAGTAGTTTGTAC	GTGCAGGGTCCGAGG

Supplementary Table 2. Summary of selected miRNAs targets for KEGG and GO analysis

let-7-5p	miR-133a	miR-328	miR-22	miR-2861	miR-518d	miR-10b-5p	miR-21	miR-125	miR-23-3p	miR-100	miR-2861	miR-518d	miR-125
HMGA2	LHFP	DRGX	C17orf58	AL627309.1	GIPC3	BDNF	ZNF367	FAM169B	ZNF225	EPDR1	AL627309.1	GIPC3	FAM169B
ARID3B	SEC61B	EIF4EBP1	CCDC67	ZNF488	APTX	ARSJ	KRIT1	DRAM2	ZNF267	AP1AR	ZNF488	APTX	DRAM2
LIN28B	TAGLN2	PGM2	KIAA0040	SPTBN5	IPO7	CRLF3	IL12A	GCNT1	PNRC2	ST6GAL-NAC4	SPTBN5	IPO7	GCNT1
FIGN	CETN3	FOXS1	GRM5	C22orf46	PTGES3L	TFAP2C	FASLG	RFXANK	TFRC	TTC39A	C22orf46	PTGES3L	RFXANK
TRIM71	FTL	CTNNBIP1	H3F3C	MRM1	SLC25A33	HOXA3	FGF18	TRIM71	AUH	HS3ST2	MRM1	SLC25A33	TRIM71
NR6A1	LDLRAP1	CHP2	NAA20	FAM83A	IGFL4	VWC2L	CCL1	NLRC5	ZNF286B	BAZ2A	FAM83A	IGFL4	NLRC5
THRSP	PTBP1	DUSP16	ZDHHC16	BZRAP1	CRYBA1	SLC6A19	GPR64	BAK1	KIAA1467	KBTBD8	BZRAP1	CRYBA1	BAK1
USP44	CLTA	CHST7	BATF3	HSPG2	TFRC	RNF186	AIM1L	SWSAP1	PPIF	FKBP5	HSPG2	TFRC	SWSAP1
FAM222B	TFAP2D	KLHL42	EIF4EBP3	SPATA33	CIB4	SOBP	PLEKHA1	NPL	PKP4	HES7	SPATA33	CIB4	NPL
IGDCC3	CELF4	EDARADD	DDIT4	XIRP1	CD33	TFRC	RSAD2	C19orf54	ZNF667	HS3ST3B1	XIRP1	CD33	C19orf54
IGF2BP1	SLC50A1	LYVE1	FUT9	FAM222B	BATF3	SMAP1	SCML2	BIN2	ZNF420	FGFR3	FAM222B	BATF3	BIN2
VSTM5	SYT2	FUBP1	PDSS1	APOC2	DHPS	KPNA5	YOD1	TSNARE1	MICU3	CTDSPL	APOC2	DHPS	TSNARE1
FZD3	TMEM200B	UBFD1	LIN7C	CHTF8	CLK4	GATA6	PELI1	RAB3D	ZNF287	RAVER2	CHTF8	CLK4	RAB3D
PXT1	TIMM17A	NF2	H3F3B	DRAXIN	IGFBP1	HCN1	TGFBI	ARID3B	SNRPC	SMARCA5	DRAXIN	IGFBP1	ARID3B
DTX2	BICC1	SNX21	NET1	TPRXL	ECHDC1	FIGN	ARMCX1	STARD13	STARD3NL	LRRC8B	TPRXL	ECHDC1	STARD13
YOD1	RBMX	NXPH3	OGN	ZNF512B	APOA2	DAZAP1	MATN2	C19orf38	PDE4B	HOXA1	ZNF512B	APOA2	C19orf38
PTAFR	VKORC1	DYNC1I1	CYTH3	LCN2	PBDC1	HOXB3	SKP2	ACHE	MRC1L1	GMPS	LCN2	PBDC1	ACHE
NGF	ZNF354A	TMEM229A	SYNE1	ANKRD23	KCTD14	NR6A1	NTF3	SLC25A35	PDE7A	MTOR	ANKRD23	KCTD14	SLC25A35
SLC52A3	SAMD5	TCF7L2	IKZF4	CEACAM19	CCDC179	KLHL29	TIMP3	SERTAD3	MRC1	NR6A1	CEACAM19	CCDC179	SERTAD3
XKR8	PRRT2	TESK2	ESR1	FAM83F	GNA14	NCOR2	BEST3	SSTR3	TOP1	FZD8	FAM83F	GNA14	SSTR3
BZW1	LASP1	NR3C1	RGS2	FIBCD1	RSL24D1	ERGIC2	SMAD7	ZFP62	RALYL	NTRK3	FIBCD1	RSL24D1	ZFP62
ARHGEF38	ZIC3	CHTF8	ASB6	PPIB	MSH5	ELOVL2	MSH2	KLF13	SNX5	TMEM30A	PPIB	MSH5	KLF13
FAM103A1	PPP2CA	RGL2	IL31	ARHGDIA	BCAP29	USP46	RNFT1	RIN3	MYH4	RASGRP3	ARHGDIA	BCAP29	RIN3
MDM4	PAX7	PIGA	ACER3	CTB-5409.9	ARL2BP	RPRD1A	SATB1	KCNIP3	PROK2	CLDN11	CTB-5409.9	ARL2BP	KCNIP3
BACH1	C12orf43	NPFFR1	ELOVL6	PLA2G2C	URGCP-MRPS24	FLJ20373	PHF14	RAD54L2	SLC25A4	TRIB2	PLA2G2C	URGCP-MRPS24	RAD54L2
C5orf51	PPP2CB	NOTCH2NL	FRAT2	FAM83G	ACSM3	SDC1	FAM13A	TOR2A	MYL12B	TRIB1	FAM83G	ACSM3	TOR2A
PAPPA	SLC30A7	RANBP10	ARRB1	EFHD2	SCNN1B	KCNA6	RP2	PPP1R12B	C3orf52	PPP3CA	EFHD2	SCNN1B	PPP1R12B
HAND1	SGMS2	SLC2A1	PRPF38A	C14orf180	HOXB3	CADM2	RTN4	TNSF4	IGSF8	ZBTB7A	C14orf180	HOXB3	TNSF4
LPGAT1	GDNF	FAM214B	CD207	MRPL28	HMGN1	FLRT2	ARHGAP24	VPS4B	BORA	GRHL1	MRPL28	HMGN1	VPS4B
TGFBR1	SUMO1	RWDD2B	FAM49B	CROCC	RB1CC1	CAMK2B	UBE2D3	NEU1	NDUFC1	TMEM135	CROCC	RB1CC1	NEU1
CDC34	FOSL2	FAXDC2	MTHFR	MBL2	REG1B	LIX1L	PPP1R3B	OSBPL9	MYH1	ST5	MBL2	REG1B	OSBPL9
ZBTB16	SIMC1	SRSF9	UNK	EPS8L3	ELOVL6	RORB	LRRC57	LFNG	WBP2	PPP1CB	EPS8L3	ELOVL6	LFNG
RNFT1	SMARCD1	ULK2	WDR82	FDX1L	TMEM42	RORA	DUSP8	SLC26A6	CCL7	NIPBL	FDX1L	TMEM42	SLC26A6
HOXB1	GPM6A	ITGA5	SLC16A14	ARHGAP19-SLIT1	UBE2I	CYTH1	PDCD4	NECAB3	ASF1A	MTMR3	ARHGAP19-SLIT1	UBE2I	NECAB3
SMIM3	DOLPP1	C16orf87	LRRC73	BSN	PIRT	SMTNL2	SOX5	EIF1AD	USP53	PI15	BSN	PIRT	EIF1AD
SALL4	PTPRZ1	EN2	A4GNT	TEAD3	SYDE2	KLF11	KBTBD7	TTPA	CCSAP	DESI2	TEAD3	SYDE2	TTPA

Aberrant circulating miRNAs in osteoporosis patients

GATM	TMEM167A	PARP16	ENO1	ALOX15B	OCIAD1	GALNT1	RMND5A	FBXW4	SATB1	INSM1	ALOX15B	OCIAD1	FBXW4
LRIG3	CMPK1	MAN1C1	CYR61	CRYAB	FGF7	GOLGA3	RAB22A	C1orf210	ARHGAP20	CEP85	CRYAB	FGF7	C1orf210
CCL7	ARPP21	MMP16	TRPM7	CLLU1OS	LPGAT1	ATCAY	PDZD8	DOCK3	DHRS11	MBNL1	CLLU1OS	LPGAT1	DOCK3
SLC35D2	PPP2R2D	ADNP	SLC35E4	ST3GAL3	WFDC12	MAP3K7	OLR1	ENTPD1	VRK3	SMARCD1	ST3GAL3	WFDC12	ENTPD1
PPP1R15B	LHX9	TRAPPC6B	C5orf24	KLK4	ZFP69B	ZNF549	SLC2A4RG	KIAA1841	C6orf62	NXF1	KLK4	ZFP69B	KIAA1841
DUSP16	SLC6A1	DDI2	NUS1	GIPC3	HNRNPC	UBE2I	SPRY1	ZNF460	NAP1L5	SLC44A1	GIPC3	HNRNPC	ZNF460
PBX3	CNN2	GBA	RFXANK	HPCA	NRCAM	TMEM183A	RASGRP1	C6orf47	C12orf23	ETV3	HPCA	NRCAM	C6orf47
TNFSF9	KIRREL	DERL2	PLCXD3	CAPNS1	CDCP2	ERI3	PFKM	TET2	RP5-1052I5.2	KDM6B	CAPNS1	CDCP2	TET2
GALNT1	XXYLT1	SHISA5	ARPC5	OBSCN	DLL3	ATXN2	S100A10	TRIAP1	MCFD2	RRAGD	OBSCN	DLL3	TRIAP1
ARID3A	LANCL2	HPCAL4	CAV3	VCX3A	NXPE3	XRN1	RALGPS2	PSMB8	SYT4	ZZEF1	VCX3A	NXPE3	PSMB8
ZC3HAV1L	TPM4	PODNL1	TRIB2	VCX3B	CCDC36	LRRC8B	GLIS2	DUS1L	PKIA	TRIM71	VCX3B	CCDC36	DUS1L
MARS2	TMOD3	PIM1	ZNF740	MAGEA11	ESM1	GABRB2	KLF5	CCNJ	VEPH1	CYP26B1	MAGEA11	ESM1	CCNJ
QARS	VPS54	HIST1H4D	ATP8A1	PDCD1	IL1RAPL1	PIK3CA	BRWD1	IRF4	HMGB2	CDYL2	PDCD1	IL1RAPL1	IRF4
LIPT2	COL25A1	SLC30A8	EMILIN3	PPP1R13B	HMGB3	CNNM4	SPRY2	BMF	APAF1	IGF1R	PPP1R13B	HMGB3	BMF
AP1S1	AGRP	USP37	ODF1	VCX	CD226	IL1RAPL1	ELF2	CDH5	C2orf69	TAOK1	VCX	CD226	CDH5
FOXP2	SGPP1	KAT6B	SCYL3	PHLDA3	SSSCA1	ZMYND11	RECK	PCTP	STX12	THAP2	PHLDA3	SSSCA1	PCTP
C8orf58	FAM57A	LNX2	MPZL3	AC092675.3	RPAIN	RAP2A	PCBP1	TMEM168	SETD8	SATB1	AC092675.3	RPAIN	TMEM168
TTC31	FOXL2	MXI1	SIRT1	GGA1	FAM213A	PTPN4	SLC16A10	PLEKHA8	MEIS1	AGO2	GGA1	FAM213A	PLEKHA8
ZBTB8B	CAPN15	HIST1H4L	YWHAZ	POP5	GINS2	IGDCC4	ST3GAL6	SLC39A9	ZNF839	BMPR2	POP5	GINS2	SLC39A9
TP53	ZNF131	USP8	CBL	CSNK2B-LY6G5B-1181	KCNV2	MDGA2	KBTBD6	OLFML2A	B3GNT1	ZNRF2	CSNK2B-LY6G5B-1181	KCNV2	OLFML2A
ZNF512B	UBA2	TP73	KCNK12	SLC25A48	CLEC3A	HAS3	PPP1R3A	HDDC3	CCNG1	ICMT	SLC25A48	CLEC3A	HDDC3
PBX1	KIF3C	GBX2	FTL	TMEM86B	ARHGAP15	ALPL	SKI	TSEN54	MYCT1	RMND5A	TMEM86B	ARHGAP15	TSEN54
GNG5	EMP2	MAP3K9	FAM83F	MED22	SPC24	NPAS3	DMRTC1B	TIFAB	ZNF23	FZD5	MED22	SPC24	TIFAB
CCNJ	EIF4A1	CA3	XXbac-BP-G32J3.20	NRM	GZMK	CECR6	STAG2	MAP2K7	RRAS2		NRM	GZMK	MAP2K7
GXYLT1	AFTPH	FOXO4	PPM1K	PRCD	ESCO2	SSX2IP	PITX2	ABTB1	ZIC4		PRCD	ESCO2	ABTB1
COIL	NRIP3	LGR4	GHRHR	NUDT2	C12orf79	ZNF367	CD69	MAP3K10	ISCA2		NUDT2	C12orf79	MAP3K10
MYCN	AL117190.3	C19orf43	SNAI1	KCNK9	CXCL11	SNX18	TADA2A	APOC4	SIX1		KCNK9	CXCL11	APOC4
GEMIN7	GABARAPL1	POLR3H	CCNJL	COL11A2	CYLC2	ONECUT1	TRAPPC8	SAMD14	ATP11C		COL11A2	CYLC2	SAMD14
DDX19B	B3GALNT1	SNRK	IL13RA1	MAEL	C1orf180	CTD-2267D19.3	CPEB3	FAM213A	CA2		MAEL	C1orf180	FAM213A
RAB15	GARNL3	HIC1	PTEN	LY9	MAP1LC3B	EPHA8	PCSK6	KHNYN	HEXIM1		LY9	MAP1LC3B	KHNYN
XRN1	RAP2C	ZNF697	COPS7B	HOXB4	ELL2	PRKAA2	SESN1	IL6R	CCM2		HOXB4	ELL2	IL6R
ADRB2	TRIM44	ESCO1	DPM2	SMIM6	AAK1	ELOVL6	PCBP2	NIPAL4	HNF4G		SMIM6	AAK1	NIPAL4
DPH3	GABPB2	TTC26	TMEM229B	C2CD4C	TERF2IP	E2F7	HRK	BAP1	CTCF		C2CD4C	TERF2IP	BAP1
SPRYD4	ELFN1	C10orf113	AC007375.1	SNX22	BCL2L2	H3F3C	BCL7A	ABHD6	NCOA2		SNX22	BCL2L2	ABHD6
AC010441.1	TXLNA	ZNF436	APBB2	SYT12	NUDT4	H3F3B	GLCCI1	TNFAIP3	SMIM18		SYT12	NUDT4	TNFAIP3
KCTD21	STOM	STT3A	RIMS4	MRPL38	TMPRSS11E	ESRRG	GABRB2	SLITRK6	ASAH2B		MRPL38	TMPRSS11E	SLITRK6
STX3	NAGS	ZNF280B	EPB41L2	COMMD9	LRRC28	BAZ1B	ARMC10	HINFP	NEK6		COMMD9	LRRC28	HINFP
ADAMTS8	ANKRD28	ARL6IP1	FBXO46	SCAMP5	SMIM11	FNBP1L	LANCL1	IER2	RAB39B		SCAMP5	SMIM11	IER2

Aberrant circulating miRNAs in osteoporosis patients

APBB3	SLC6A6	WASF2	LGALS1	FMO4	DCTPP1	PAPD5	PAN3	MAVS	MAP7		FMO4	DCTPP1	MAVS
DDX19A	CRTAM	PTPN9	IL17RD	NT5C	GRWD1	TBX5	ST6GAL1	TSTA3	RCHY1		NT5C	GRWD1	TSTA3
MED8	ZC3H11A	NKPD1	KLF6	AFAP1L2	TMEM170B	CSRNP3	ASF1A	SEMA4D	SPTSSB		AFAP1L2	TMEM170B	SEMA4D
CDC25A	PLEKHA3	DNAH10OS	ANKRD13A	GLOD5	GALNT11	BBX	RBPJ	KCTD15	SH3BGR		GLOD5	GALNT11	KCTD15
CCND2	SFXN2	SOGA1	GATM	DPYSL4	LILRA1	FAM196A	PBRM1	MTF1	RGS8		DPYSL4	LILRA1	MTF1
E2F6	DCLRE1A	PEF1	CENPV	ELAVL3	TMEM116	PRRT3	JHDM1D	SH3TC2	TPST1		ELAVL3	TMEM116	SH3TC2
CRCT1	PFAS	RSBN1L	DAW1	TCEAL6	KLRB1	IGSF1	JAG1	GJC1	NACC2		TCEAL6	KLRB1	GJC1
FAS	KIAA1429	MPV17	AK2	NHLRC4	STARD4	ACTG1	MAP2K3	KCNK10	STXBP6		NHLRC4	STARD4	KCNK10
KLHDC8B	QKI	MBNL3	NHP2	LEMD2	PATE1	EPHA2	GRAMD3	GMIP	YOD1		LEMD2	PATE1	GMIP
PSORS1C2	MAEA	LHFPL2	DNAJB5	TCEAL3	FUT1	KIAA0247	CHIC1	PODXL	CCDC82		TCEAL3	FUT1	PODXL
UFM1	TBPL1	SLC27A4	TYRO3	CAND2	MBLAC2	MDGA2	TMEM170A	NR6A1	FUT4		CAND2	MBLAC2	NR6A1
ZNF710	SF3B4	NRIP1	ANKHD1-EIF4EBP3	KIAA1279	EGLN3	HNRNPK	DCAF7	SLC25A15	FBN2		KIAA1279	EGLN3	SLC25A15
ATPAF1	TMEM170B	KIF2A	CDX2	KLK14	C10orf11	JARID2	HIPK3	LRRC10B	GLB1L3		KLK14	C10orf11	LRRC10B
GNPTAB	SOX4	ITGA9	LRCH1	FAM131B	CALM1	KCTD16	TIAM1	LIN28B	CFL2		FAM131B	CALM1	LIN28B
CPEB2	TSPAN18	ZC3H12B	CSF1R	UBE2F	ZNF80	KLF7	OSR1	UBE2G1	KIAA0922		UBE2F	ZNF80	UBE2G1
CPA4	GCH1	HIF1AN	FBXL19	MAP3K6	RNF41	PALM2	MAP3K1	SBNO1	CLDN14		MAP3K6	RNF41	SBNO1
BEND4	RBMXL1	METTL21B	ERBB3	YKT6	CCDC91	WWC2	C10orf12	PSTPIP2	SYS1		YKT6	CCDC91	PSTPIP2
PEX11B	DCBLD1	ACSS2	BTG1	CLN6	TIMELESS	NR4A3	CASKIN1	RS1	TOX3		CLN6	TIMELESS	RS1
PARD6B	SH3GL2	YWHAZ	VASP	RAB15	MOB1B	NEDD4	MBLAC2	CGREF1	KIAA1107		RAB15	MOB1B	CGREF1
PQLC2	ZNF280C	PTPRU	TRUB1	LTA	LRRC63	BCL6	DAZL	ATP10D	A1BG		LTA	LRRC63	ATP10D
SLC25A18	SLC39A1	H2AFX	CATSPERG	KRT35	THTPA	DOCK11	NFIB	MAPK12	UQCRFS1		KRT35	THTPA	MAPK12
TMEM234	METTL21B	HAP1	LZIC	ESYT1	MORC1	RNF165	XKR6	C17orf103	NR6A1		ESYT1	MORC1	C17orf103
NEK3	FOXC1	MICALL1	RBM15	MSI1	SMEK2	RP6-24A23.6	ERG	SAMD10	FRA10AC1		MSI1	SMEK2	SAMD10
TTLL4	PTPRK	C6orf223	NCOA1	MTSS1L	TEKT1	CTNNBIP1	ALX1	KCNS3	ACVR1C		MTSS1L	TEKT1	KCNS3
KCTD17	WASF2	SHKBP1	DPY30	PAX5	LYRM7	WBP11	PLAG1	ARID3A	TMED5		PAX5	LYRM7	ARID3A
SLC5A9	RAVER1	FAM199X	NTRK2	ANKRD24	KCNJ14	TRIM2	CNTFR	SYT2	PDCL3		ANKRD24	KCNJ14	SYT2